





Article

Corrosion Resistance Performance of Epoxy Coatings Incorporated with Unmilled Micro Aluminium Pigments

Ubair Abdus Samad ¹, Mohammad Asif Alam ¹, Asiful H. Seikh ^{1,*}, Jabair A. Mohammed ¹,
Saeed M. Al-Zahrani ² and El-Sayed M. Sherif ^{1,*}

¹ Center of Excellence for Research in Engineering Materials (CEREM), Deanship of Scientific Research, King Saud University, P.O. Box 800, Riyadh 11421, Saudi Arabia

² Department of Chemical Engineering, College of Engineering, King Saud University, P.O. Box 800, Riyadh 11421, Saudi Arabia

* Correspondence: aseikh@ksu.edu.sa (A.H.S.); esherif@ksu.edu.sa (E.-S.M.S.)

Abstract: The current work is in continuation of our previous work where we reported changes in the properties of epoxy coatings using two different types of hardener in different stoichiometric ratios. The best results-oriented coating stoichiometry was then taken in this research for further modification with the incorporation of 1, 2 and 3 wt.% micro aluminium (Al) pigments designed for coating carbon steel panels. After 7 d of curing, the coated panels were characterized using X-ray diffraction (XRD), (SEM) scanning electron microscopy, (TGA) thermogravimetric analysis, pendulum hardness, a scratch test and nano-indentation. Electrochemical tests were carried out for various exposure periods of time, i.e., 1 h, 7 d, 14 d, 21 d and 30 d, in a 3.5% sodium chloride (NaCl) solution. For the coatings, we found that the presence of 1% Al provided the highest corrosion resistance after exposure periods in the NaCl solution. We also found that prolonging the immersion time decreases the corrosion resistance after 7 d, but increasing the time of immersion to longer periods (14 d, 21 d and 30 d) enhances the corrosion resistance and reduces the degradation of the coatings.

Keywords: epoxy coatings; aluminium powder; corrosion; nanoindentation; electrochemical techniques



Citation: Abdus Samad, U.; Alam, M.A.; Seikh, A.H.; Mohammed, J.A.; Al-Zahrani, S.M.; Sherif, E.-S.M. Corrosion Resistance Performance of Epoxy Coatings Incorporated with Unmilled Micro Aluminium Pigments. *Crystals* **2023**, *13*, 558. <https://doi.org/10.3390/cryst13040558>

Academic Editors: Dah-Shyang Tsai and Ayman H. Ahmed

Received: 9 February 2023

Revised: 16 March 2023

Accepted: 20 March 2023

Published: 24 March 2023



Copyright: © 2023 by the authors. Licensee MDPI, Basel, Switzerland. This article is an open access article distributed under the terms and conditions of the Creative Commons Attribution (CC BY) license (<https://creativecommons.org/licenses/by/4.0/>).

1. Introduction

Coatings play an important role in protecting metallic structures or substrates from corrosion and are currently used excessively in various industries such as automotive, power generation, aerospace and oil production [1,2]. There has been considerable interest in the last decade in the development of new coating formulations to improve their barrier and corrosion protection properties. Of the various coating systems currently in use, epoxy-based coatings are the best known [3,4]. This is because they have high resistance to chemical agents, good insulation and excellent adhesion properties [5]. However, the limitations of epoxy-based coatings are their brittleness, which leads to failures due to mechanical abrasion [6]. Initially, they have good barrier properties against corrosive environments. However, when epoxy coatings are exposed to long-term corrosive environments, significant hydrolytic degradation occurs. This leads to significant corrosion of the metallic substrates and delamination of the coatings [7].

The development of new coating formulations has motivated researchers in industrial and academic organizations to improve the performance and/or minimize the content of volatile organic compounds (VOC) in existing epoxy coatings [8]. The adhesion barrier properties and corrosion protection properties of the epoxy coating systems can be further improved by adding suitable pigments and additives [9]. The improvement of the corrosion protection performance of the epoxy systems depends on the type, distribution, volume fraction and compatibility of the pigment used in the epoxy coating. It is also believed that the addition of these pigments forms an oxide layer of corrosion-inhibiting compounds with the epoxy, thereby protecting the metallic substrates. However, despite their efficiency in

protecting against corrosion, a decrease in impact and abrasion resistance has been observed with the addition of these pigments [10]. In addition, the pigments are considered toxic and pose a significant risk to the environment. Recently, the use of nanosized pigments has been preferred over micro sized pigments because the reduction in particle size improves the interface between the particles and the coating matrix [11]. It has also been observed that the nanocomposite coatings have improved corrosion resistance and barrier properties compared to conventional coatings with micron-sized particles [12]. Commonly used metallic pigments include aluminium [13], zinc [6] Zn-Ni [14] and Zn-Ni-Al₂O₃ [15] in powder form. The incorporation of these metallic nanoparticles into the epoxy coatings leads to the development of environmentally friendly coatings. These nanoparticles occupy the small voids created by local shrinkage during curing of the epoxy coating. This leads to a significant improvement in the barrier properties of the nano-pigmented coatings [16].

Recent advances in nanocomposite coatings include the production of aluminium-containing coatings to improve corrosion resistance in highly corrosive environments [17]. The Al particles have a greater tendency to react with water and form aluminium oxide and aluminium hydroxide layers on the outside of the coating surface. These layers protect the metallic substrate and increase the corrosion resistance of the coatings [18]. Al as a pigment in an epoxy matrix is currently used in the automotive, plastics, ink and paint industries exclusively for its glossy appearance, excellent scratch resistance, improved electrical and mechanical properties and optimal cost [19]. González et al. studied the effect of aluminium powder on the corrosion resistance of epoxy coating. It has also been observed that the precipitation of corrosion products on the steel surface in the presence of Al powder can lead to an increase in the corrosion resistance of the epoxy coating [13]. It is also reported in the literature that the addition of Al pigment to a zinc-rich coating leads to an increase in corrosion resistance with a simultaneous decrease in cathodic sacrificial behaviour [20,21]. The corrosion resistance of nano-composite epoxy coatings by incorporating nano-Al pigment into epoxy resin was investigated, and it was found that the nano-Al pigment initially corroded to form alumina and aluminium hydroxide layers, which hindered the transfer of corrosion fluid into the coatings, thereby increasing the corrosion resistance of the developed coatings [22,23].

This work is in continuation of our previous published work [24] where we studied the behaviour of epoxy and two different types of hardeners in varying stoichiometric ratios. Here, we took the best performing epoxy formulation and studied its behaviour with the incorporation of Al particles. The micro Al pigments (1, 2 and 3) wt.% were added into an epoxy coating composed of diglycidyl ether of bisphenol-A (DGEBA), which was then amine-cured. A suitable coupling agent must be used in order to disperse microparticles in the epoxy matrix in a homogeneous and de-agglomerated manner. The final coating composition was applied to the metal substrate and several methods were used to characterize it. FE-SEM was used to analyse the coating formulations both before and after the addition of Al pigments. Mechanical properties were evaluated by means of nano-indentation. Finally, EIS techniques were used to investigate the coated substrates' corrosion resistance characteristics.

2. Materials and Methods

The formulations were prepared by first taking a small quantity of acetone in a beaker for the surface treatment of as-received 2 microns of Al powder (Alfa aesar, Haverhill, MA, USA, 99.5%) using the sonication technique. For this purpose, the calculated amount of Al powder was taken as presented in Table 1 and dried using a vacuum oven prior to its addition at 100 °C for 24 h. This process includes the use of methyl isobutyl ketone (MIBK, Ideal Chemicals, Riyadh, KSA) and xylene (Merck, Rahway, NJ, USA, 99%) as organic solvents in the presence of an air-releasing agent. The amount of silane to facilitate the dispersion of particles in matrix resin (see Table 1) was added dropwise to acetone under continued sonication for 3 min. After that, the Al powder was added to the acetone (little by little) and the process of sonication was continued for 15 min. On the other hand, the

calculated epoxy resin was taken in a clean beaker; then, resin was diluted with xylene using the mechanical mixer in order to achieve the proper dispersion of Al particles after their addition. Prior to the addition of the particles, the stated additives were added in the diluted epoxy bisphenol A diglycidyl ether epoxy resin (DGEBA, Hexion Chemicals, Columbus, OH, USA) matrix until homogeneity was achieved. In the meantime, and after finishing the sonication process, the treated particles were added to the diluted epoxy resin and grinded mechanically using a high-speed mechanical mixer at 5000 RPM, in order to facilitate the proper mixing of the particles as well as the removal of excess solvent from the system. After the completion of mixing, the formulation was degassed for the removal of excess solvent and trapped air inside the formulation. After degassing, the formulation was left for stabilization for 10 min at room temperature. The calculated amount of hardener polyamidoamine adducts ARADUR 450 (PA450, Huntsman Advanced Materials, Woodlands, TX, USA) was then added to the prepared formulation and applied to the metal substrates for the purpose of characterization using a bird applicator (gap size of 120 μm) with the help of a sheen automatic film applicator. All the formulating ingredients along with their respective percentages are described in Table 1.

Table 1. Epoxy formulating ingredients for the fabricated coatings containing Al particles.

Sample Code	Epoxy (gm)	MIBK (mL)	Xylene (mL)	Silane	Al wt. %	Dispersing Additive	Levelling Agent	Air Release Additive	PA-450 (gm)
Al-1	83.34	8	8	2.0	1.0	1.0	1.0	1.0	15.90
Al-2	83.34	8	8	2.0	2.0	1.0	1.0	1.0	15.90
Al-3	83.34	8	8	2.0	3.0	1.0	1.0	1.0	15.90

The samples to be coated were degreased with the help of acetone before the application of the prepared coating. Glass samples were coated for pendulum hardness and metal panels of different sizes were coated for mechanical, electrochemical and nanoindentation characterization. The sample after coatings were left for curing and, after 7 d of complete curing, characterizations were performed.

The coated panels were measured after 7 d to determine the ideal mix of mechanical and electrochemical qualities. TGA was used to analyse the thermal characteristics of the coatings (SDT Q600, TA Instruments, New Castle, DE, USA). Utilizing SEM, the morphology of the coatings was examined (scanning electron microscope, Joel, Tokyo, Japan). With the aid of traditional testing methods such as pendulum hardness (ASTM D-4366), impact resistance (ASTM D-2794) and scratch testing (ASTM D-7027), the mechanical characteristics of the produced coatings were examined. By counting the number of oscillations on the surfaces of the coatings, the pendulum hardness (Koenig pendulum tester: model 707/K, Sheen, Surrey, UK) was used to determine the surface hardness of the coatings; higher oscillations correlated with higher surface hardness. By dropping a standard weight on the surface of the coating from various heights, the impact strength (Gardner impact tester: model IG-1120, BYK, Columbia, SC, USA) was determined. Impact failure is regarded as happening at the height at which the coating ruptures. By increasing the weight against a moveable mounting platform where the samples were attached, the scratch resistance (scratch tester: model 705, Sheen, Surrey, UK) was determined. Starting from 500 g to a maximum of 10 kg, the load was gradually increased. The failure is the weight at which the coating breaks. With the use of the nano test platform 3 from micromaterials, the nanomechanical characteristics of the coatings were examined. The qualities of the coating were examined using a load control program and a Berkovich (Micromaterials, Wrexham, UK) type indenter. A maximum load of 250 mN was applied to the coatings at a loading rate of 1 mN/s. Upon reaching the maximum load, the load was held for 60 s to remove anomalies related to creep. Following that, the load was entirely removed at a rate of 1 mN/s. On each sample, at least five indentations were made in various places, and the findings are shown as an average. Using a conventional 3-electrode cell and Autolab Ecochemie PGSTAT 30 (Metrohm, Amsterdam, The Netherlands), electrochemical impedance spectroscopy (EIS)

was carried out. Prior to testing, the coatings were exposed to a 3.5% NaCl solution for periods ranging from 1 h to a maximum of 30 d. The EIS experiments were carried out at a frequency ranging from 100,000 to 0.1 Hz by applying a ± 5 mV amplitude sinusoidal wave perturbation at the corrosion potential.

3. Results and Discussion

3.1. Thermogravimetric Analysis (TGA)

In order to determine the thermal properties of epoxy coatings with the addition of aluminium particles in different percentages, the prepared coatings were subjected to heating from ambient temperature up to 600 °C under a N₂ environment. The obtained graphs are shown in the figures below.

From Figure 1, analogous degradation curves can be witnessed for the prepared coating samples with the increasing percentage of Al particles. This typical profile is observed because of epoxy, which is the main matrix of coatings [25,26]. The initial degradation of the coating samples started above 100 °C, while the major decomposition or burning of epoxy resin started approximately above 350 °C. The initial decomposition happened because of trapped diluents and probably unreacted reaction components, while the major decomposition was because of the epoxy chain burning with increasing temperature.

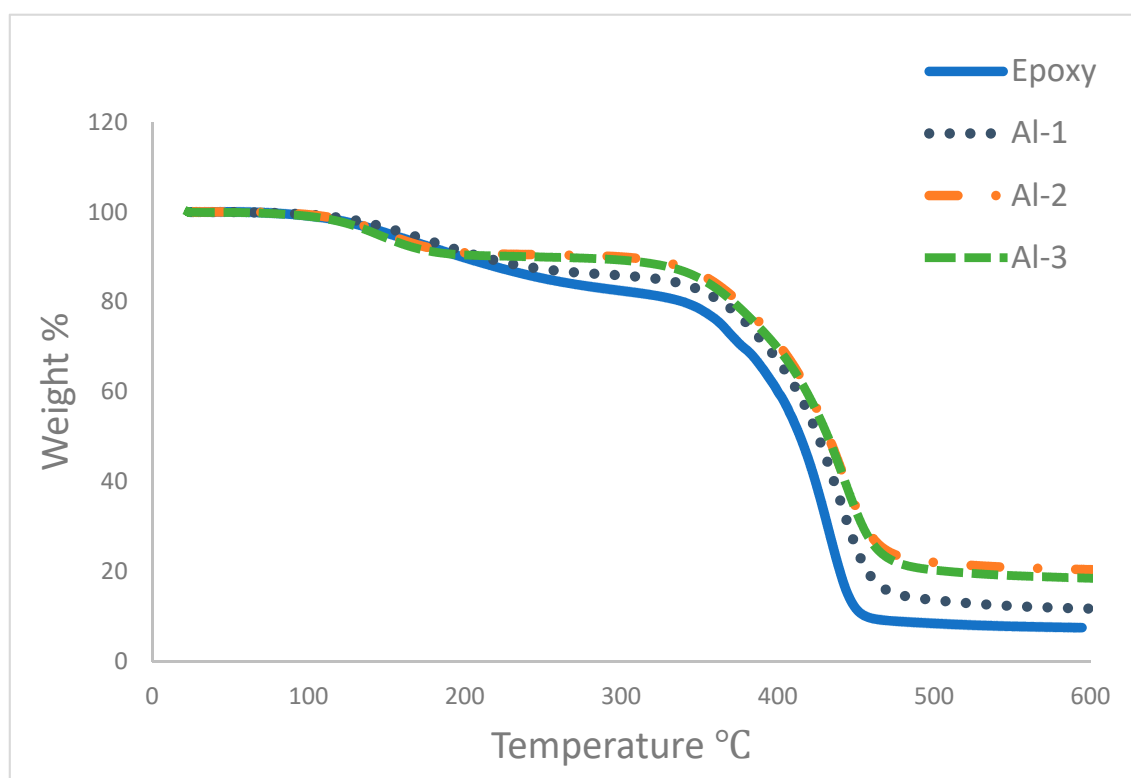


Figure 1. TGA curves obtained neat epoxy coating as well as with different loading proportions of micro Al powder.

The micro Al particle addition in resin improved the thermal properties of base epoxy resin. In comparison to the results obtained for base epoxy coating, as presented in Table 2, an increase of 36% is reported in the initial decomposition temperature at 15% weight loss, while an increase of approximately 3.5% in temperature is also witnessed at 75% weight loss. The obtained temperatures at 15%, 25%, 50% and 75% weight loss are presented in Table 2.

Table 2. Temperatures at various percentages of weight loss.

Sample Name	T 15%	25%	50%	75%	Residue
Epoxy	240.22	360.54	413.03	435.24	7.88
Al-1	325.72	380.73	425.91	450.44	10.82
Al-2	356.45	389.58	432.5	468.23	19.54
Al-3	351.55	386.34	432.02	463.61	17.22

3.2. Field Emission Scanning Electron Microscope (FE-SEM)

The morphology of the epoxy-coated samples with the addition of Al particles were investigated under a scanning electron microscope. The obtained SEM images for the AL-coated sample with 2% Al are shown in Figure 2. It can be seen in Figure 2 that there is good distribution of Al particles on the coating's surface. The EDX analysis also proves the good distribution of Al particles seen on the coated surface. As the coating consisted of a hydrocarbon chain, the presence of carbon was the highest in the sample.

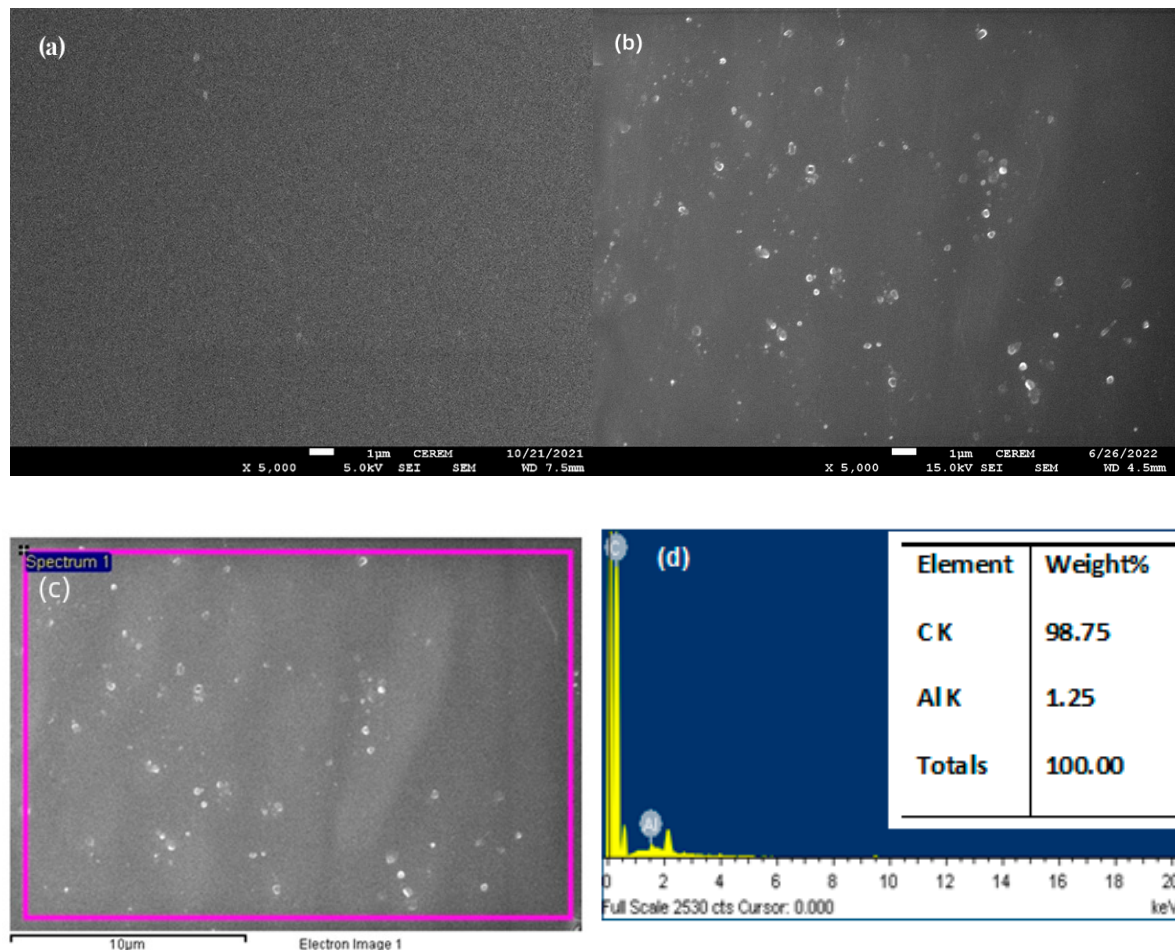


Figure 2. SEM images of neat epoxy-coated (a) and 1% Al-coated (b) samples along with EDX elemental analysis (c,d).

3.3. XRD Analysis

An XRD analysis of the coating samples was performed using Bruker-DiscoverD8, with Cu $\text{K}\alpha$ (1.542 \AA). The XRD patterns of coatings with additives of Al powders are illustrated in Figure 3 below. The peaks were measured in the range of 5–90 degrees at a scan rate of 2 deg/min. The existence of the initial broad peak in the 2 θ region of 15–25 degrees indicates the amorphous characteristic of the epoxy; this characteristic peak position of the coating remained unchanged even after the addition of the aluminium

particles, implying that no structural changes occur in coatings as a result of the presence of additives. Distinctive Al peaks are also seen in the XRD pattern.

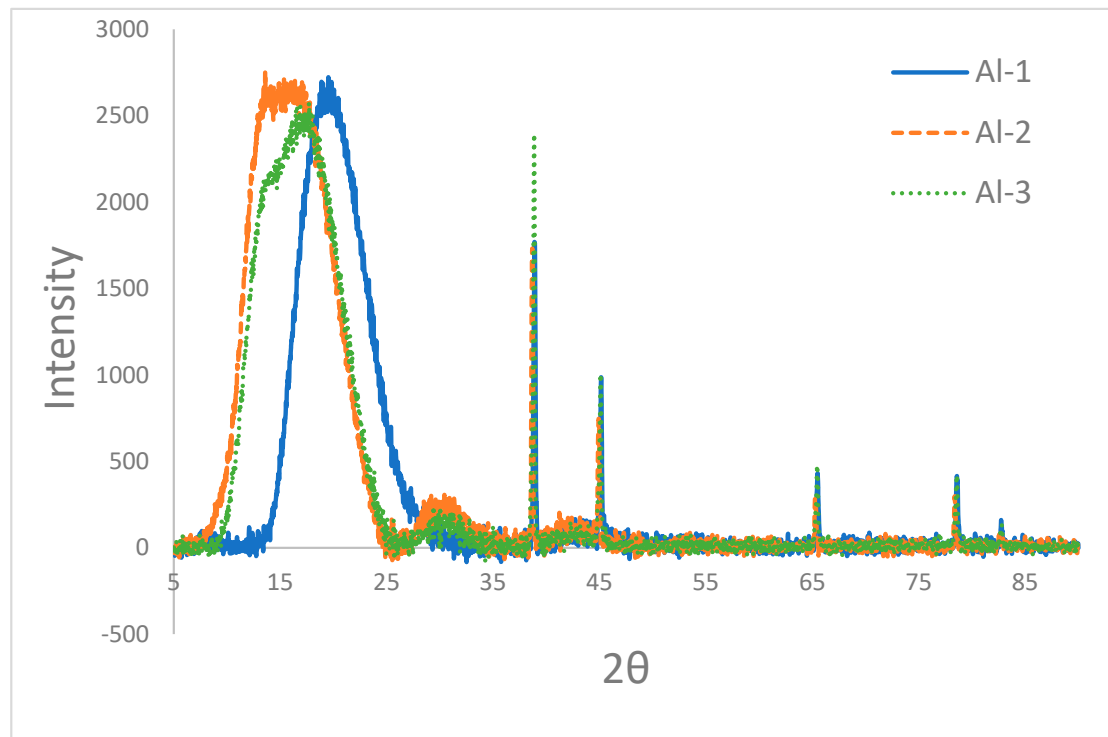


Figure 3. XRD graph for coatings prepared with the different percentages of micro Al powder.

3.4. Mechanical Properties

The mechanical characterizations, such as surface hardness (pendulum), resistance to scratch and impact, were measured in order to study the effect of different percentages of Al particles on the final properties of the coatings. The results obtained from the mentioned mechanical characterizations are presented in Table 3.

Table 3. Obtained results on the fabricated epoxy coatings containing different Al particles.

Sample Code	Dry Film Thickness (μm)	Number of Oscillations	Failure Load (Kg)	Impact Resistance (lb/in ²)
Epoxy	100 ± 10	159	5.5	48
Al-1	100 ± 10	164	5	48
Al-2	100 ± 10	170	5.5	48
Al-3	100 ± 10	176	6	64

The hardness of the coating is directly proportional to the oscillations. This means that the number of oscillations increases with the increased hardness of the coatings.

The results shown in Table 3 and the graphical illustration in Figure 4 show the properties of the coatings, suggesting an increment in mechanical properties with the increase in particle percentage. The incarnation of Al particles in 3 wt.% yields the maximum numbers where the addition of particles increases the properties in all domains of testing. This increase in coating properties is because of the higher interaction of added particles with the resin. It has been reported in the literature that under a certain limit, the added fillers tend to increase the coating properties [27–29].

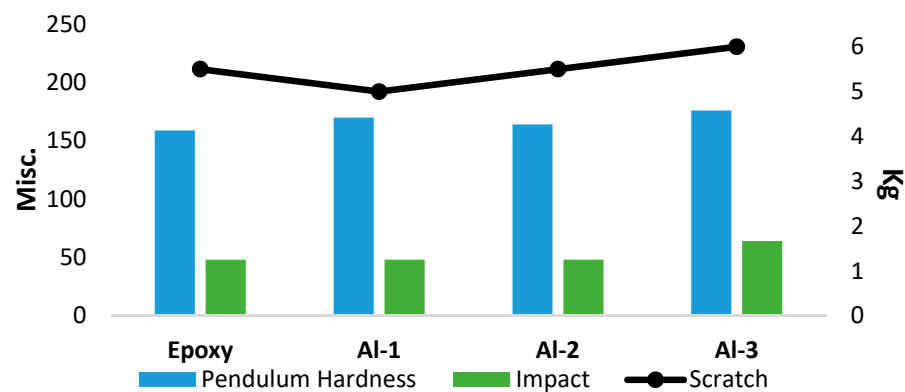


Figure 4. Graphical representation of the coating's obtained mechanical properties.

3.5. Nanoindentation Analysis

The prepared coatings' elastic modulus and hardness with three different percentages of Al particles added to epoxy coatings were analysed using the indentation. A nano-indenter manufactured from micromaterials was used to test the coating properties. To obtain consistency in the analysis, every sample was tested with six indentations at different locations across the sample, and the obtained results are shown as an average.

Figure 5 depicts typical load vs. displacement curves for epoxy coatings modified with Al particles, with a maximum load of 250 mN. There were no discontinuities observed in the loading cycle, which suggests that no cracks were created during the loading phase of the indentation. Figure 5 demonstrates how the resistance to indentation force for varied formulations increased while using analogous testing parameters. The inclusion of Al particles to the epoxy system improved the resistance to indentation force. The load vs. displacement curves shift to lower values of depth, indicating an increase in coating strength (see Figure 5).

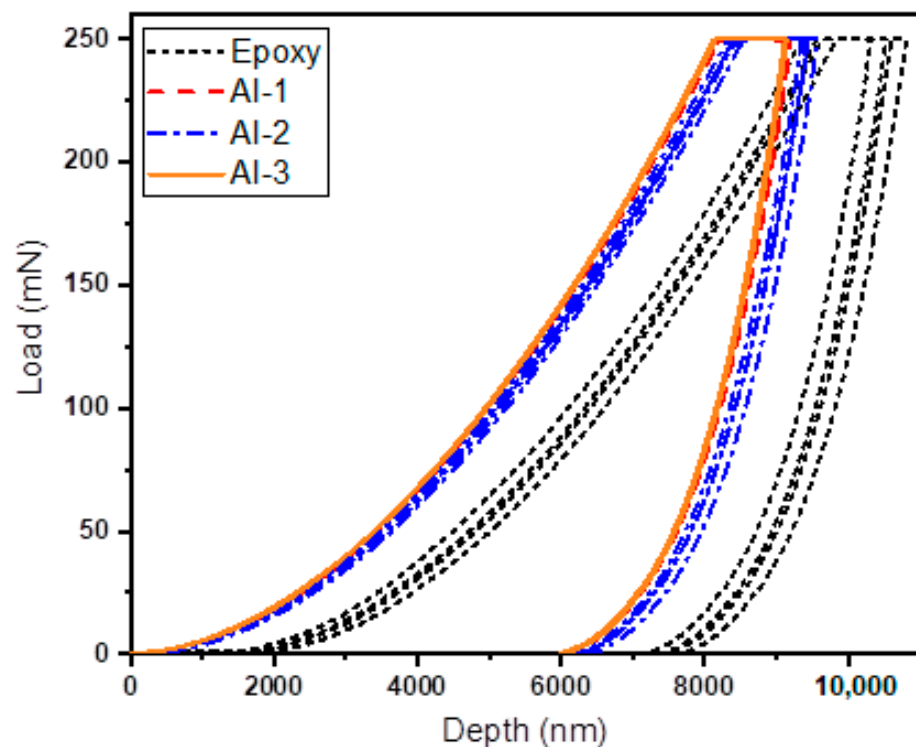


Figure 5. Obtained indentation curves for neat epoxy as well as with the Al particles in different percentages.

The samples were subjected to indentation examination using built-in machine software from Micro Material in order to determine the samples' modulus and hardness. The Oliver and Pharr [30] method is used by this software to calculate the coatings' hardness and modulus. Figure 5 shows the indentation load vs. depth curve for epoxy coatings loaded with micro aluminium in altered amounts. The results obtained are shown in Table 4.

Table 4. Indentation hardness and modulus for the coatings prepared from the different Al particles.

Sample Code	Hardness (GPa)	Modulus (GPa)
Epoxy	0.120	3.3
Al-1	0.146	3.6
Al-2	0.156	4.0
Al-3	0.153	3.8

The impact of Al particles on elastic modulus and indentation hardness at 250 mN is depicted in Figure 6. With the addition of particles at various percentages, it can be seen that the hardness and modulus both increased in comparison to the base epoxy coating without any filler [24]. With the addition of 2% Al particles, the highest values of indentation hardness were recorded. Table 4 provides the hardness and elastic modulus values.

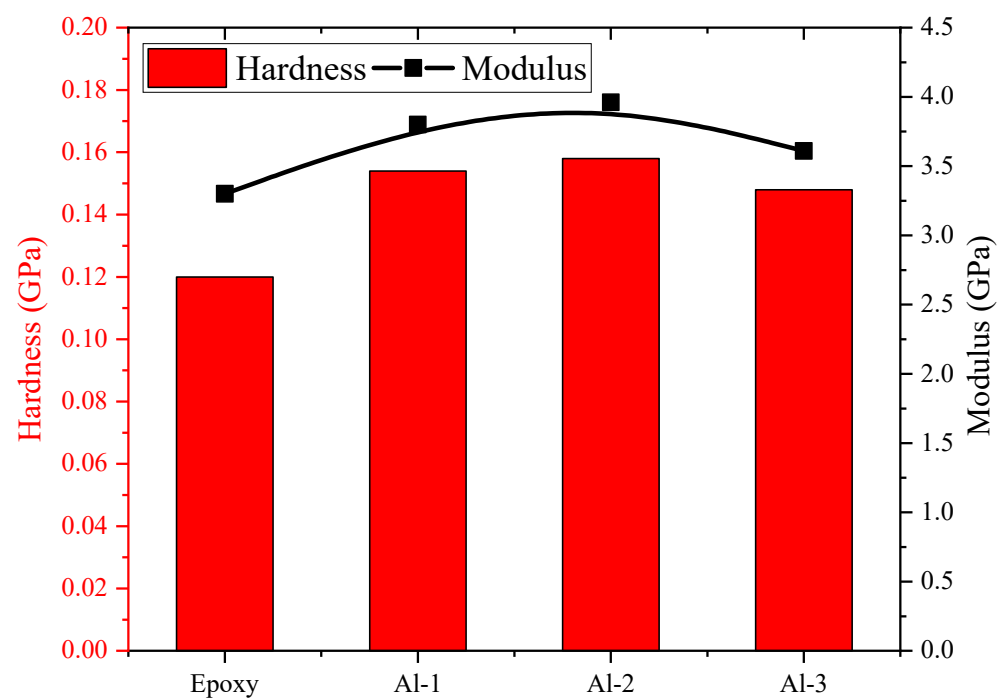


Figure 6. Graphical representation of the coating's obtained hardness and modulus.

The obtained results show that the addition of particles tends to improve the hardness of coatings due to their inclusion in matrix resin and influence on crosslink ability. The increase in elastic modulus with the addition of Al particles suggests increased toughening. The use of fillers increases hardness due to their adherence with matrix resin, which in turn increases the crosslink density of cured coatings. Furthermore, the inclusion of filler is responsible for limiting chain mobility during the curing phase, hence limiting disaggregation [7,31]. The results of the indentation study are consistent with the findings of other conventional mechanical investigations in which the addition of Al particles improved pendulum hardness and scratch resistance. It is of great interest to see the analysis of conventional mechanical testing, where an increase in impact strength was witnessed with the increasing percentage particles. Meanwhile, the results obtained from

the nanoindentation analysis suggest an increase in modulus, which is highly unlikely. Studies on this type of investigation with the addition of metal powders suggest otherwise, where the addition of metallic powder as filler into the matrix, in the case of an increase in modulus, reports a decrease in impact strength [32,33]. The addition of Al particles in the resin acts like a toughening agent where the modulus and impact simultaneously increase [34].

3.6. Electrochemical Impedance Spectroscopy (EIS) Results

The EIS technique has been widely utilized to investigate the corrosion and its mitigation as a powerful method [35–42]. The Nyquist plots for the different coatings are displayed in Figure 7 for the coatings after their immersion in 3.5% NaCl solutions for (a) 1 h, (b) 7 d, (c) 14 d, (d) 21 d and (e) 30 d, respectively. These data were also fitted to a best equivalent circuit, which is shown in Figure 7f. The values obtained from this circuit are registered in Table 5. The Nyquist spectra of 1%, 2% and 3% in all EIS figures refer to 1% Al, 2% Al and 3% Al, respectively, as indicated in Table 1 by Al-1, Al-2 and Al-3, for the fabricated coatings.

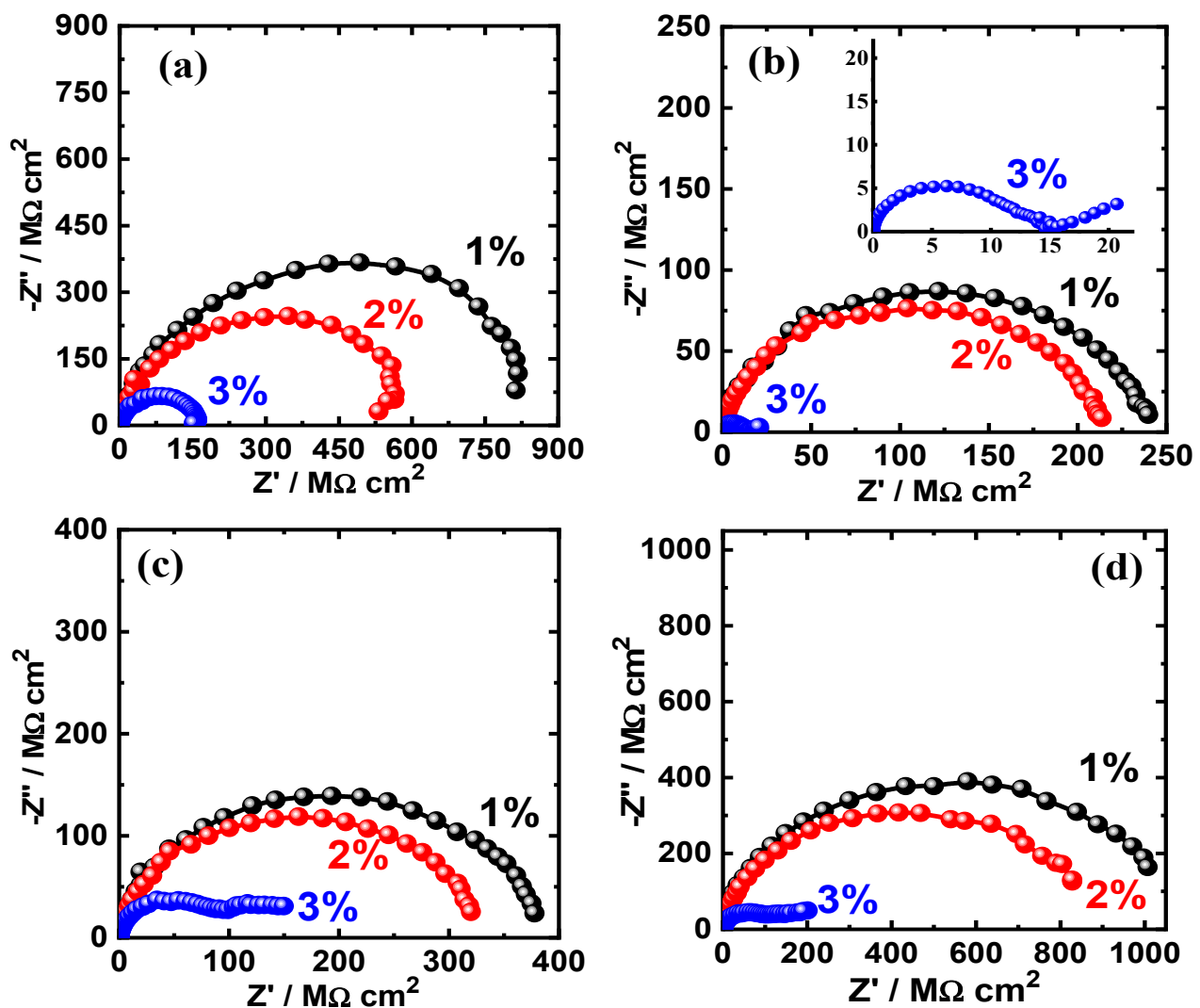


Figure 7. Cont.

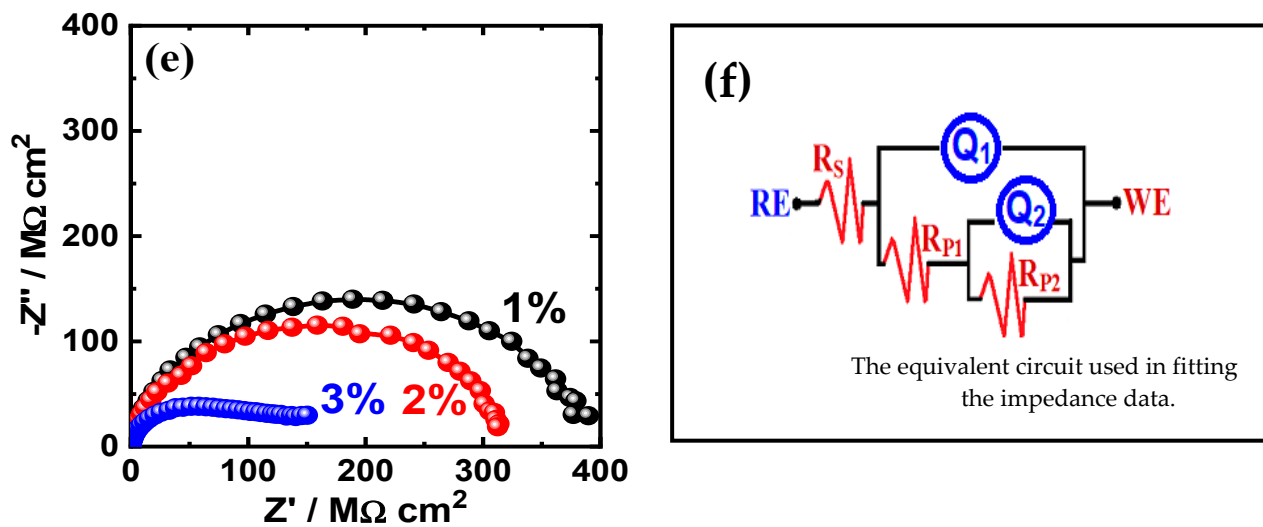


Figure 7. Nyquist plots for the coating that contains 1% Al, 2% Al and 3% Al after exposure to 3.5% NaCl solution for (a) 1 h, (b) 7 d, (c) 14 d, (d) 21 d and (e) 30 d, respectively; (f) shows the circuit model used to fit the obtained EIS data.

Table 5. Parameters obtained from fitting the impedance data.

	$R_s/\Omega\text{ cm}^2$	Q1		$R_{p1}/M\Omega\text{ cm}^2$	Q2		$R_{p2}/M\Omega\text{ cm}^2$
		$Y_{Q1}/F\text{ cm}^{-2}$	n		$Y_{Q2}/F\text{ cm}^{-2}$	n	
Al-1 (1 h)	158	0.000818	0.97	1538	0.000814	0.68	7586
Al-2 (1 h)	142	0.000934	0.96	1350	0.001072	0.80	4164
Al-3 (1 h)	135	0.000981	0.90	123	0.001084	0.72	1643
Al-1 (7 d)	131	0.000965	0.97	3736	0.001662	0.59	2121
Al-2 (7 d)	127	0.001288	0.93	198.0	0.003962	0.19	1836
Al-3 (7 d)	102	0.001006	0.97	0.4041	0.095990	0.12	1065
Al-1 (14 d)	112	0.000924	0.98	388.8	0.000245	0.58	3649
Al-2 (14 d)	98	0.008549	0.98	291.2	0.001305	0.57	3203
Al-3 (14 d)	89	0.001029	0.97	162.8	0.001179	0.17	2125
Al-1 (21 d)	104	0.0008742	0.98	686.9	0.008166	0.54	1108
Al-2 (21 d)	100	0.0008222	0.98	6934	0.0009125	0.54	883.4
Al-3 (21 d)	93	0.0009863	0.97	4586	0.001050	0.31	452.7
Al-1 (30 d)	99	0.0013180	0.93	353.1	0.002381	0.33	404.8
Al-2 (30 d)	92	0.0009002	0.97	496.2	0.001555	0.59	248.4
Al-3 (30 d)	86	0.006135	0.94	99.9	0.009880	0.97	228.7

It is seen from Figure 7b that the Nyquist plots obtained for the coating that contains only 1% Al show the widest diameter of the obtained semicircle. This reveals that adding 1% Al gives the coating higher corrosion resistance as compared to adding higher Al percentages. This was indicated by the obtained Nyquist plots for the coatings that contain 2% Al and 3% Al, where increasing the Al% decreases the diameter of the obtained semicircle. This confirms that only 1% Al included in the coating is the best to maintain the higher performance obtained for the coating in the solution for 1 h, while increasing the content of Al is undesirable in regard to the corrosion resistance as well as the cost of the prepared coatings.

Prolonging the period of exposure time for the coatings to 7 d in the chloride solution (3.5% NaCl) is clearly seen to decrease the corrosion resistance for all the collected Nyquist plots that are shown in Figure 7b. The decrease in the overall diameter for all samples is most probably due to the degradation of the coatings with time, as compared to the plots shown in Figure 7a that were obtained after only 1 h immersion. However, and under the same condition, the Nyquist plot obtained for the coating that contains 1% Al still shows the

best performance with the highest corrosion resistance. This confirms the result that only 1% Al is enough and perfect to obtain the maximum corrosion resistance for our fabricated coatings, even after 7 d of their exposure to the corrosive sodium chloride solution.

Further prolonging the time of exposure of the fabricated coatings in the chloride solution to 14 d before the EIS measurements resulted in the Nyquist plots that are presented in Figure 7c. It is clear that the plots show a similar behaviour to those obtained after 1 h (Figure 7a) and 7 d (Figure 7b), indicating that the coatings are well manufactured and prepared. Here, the plots obtained after 14 d show values that are a little higher than those obtained after 7 d of the samples' immersion, but still lower than those obtained after only 1 h immersion. This is due to the formation of a corrosion product layer with the increase in time that led to protecting the surface of the coating and offering this relatively higher corrosion resistance as compared to the plots obtained after 7 d. This can also lead to a partial degradation of the coatings with higher resistance to corrosion in the sodium chloride solution with time [43–45]. The obtained results after 14 d of the exposure before measurement thus and again confirm that 1% Al gives the best result for a coating with the best corrosion resistance, which gives a better cost-effective coating.

The Nyquist plots that were obtained after 21 d of the exposure of the different coatings to the test corrosive solution are depicted in Figure 7d. It is obvious that all coatings show a similar behaviour to those plots obtained after shorter exposure periods. The only difference that is recorded for all coating samples is that the diameter of the obtained semicircles is wider, confirming that after 21 d, the corrosion resistance increased for all fabricated coatings. This indicates that increasing the immersion time for the coatings in the chloride solution under this condition allows the surface of the coatings to develop a layer of corrosion products that prevent its degradations, and thus, increases its corrosion resistance to the highest [46–49]. As is the case for all immersion times, the coating that contains only 1% Al shows the widest diameter for its semicircle, as well as showing the highest values for the real and imaginary resistances, which proves the ability of this low % to be sufficient and that there is no to increase the Al % within the coating to 2% or 3%.

Within the longest period of exposure time (30 d, as seen in Figure 7f), the coatings show a similar behaviour but with somewhat smaller diameters for the obtained semicircles of the Nyquist plots. This might be expected, where the formed corrosion product was not fully able to protect the surface from degradation after such a long period (30 d) of exposure. However, the fabricated coating with only 1% Al shows the best performance, as indicated by the highest values of both real and imaginary resistances being recorded for it. This was also confirmed by the values of the resistances R_s , R_{p1} and R_{p2} , which recorded the highest values in the presence of 1% Al nanoparticles. Moreover, the values of Q_1 with their n values close to unity refer to double-layer capacitors with little pores; these Q_1 s recorded the lowest values when 1% Al was present within the coating. The obtained results for the coatings with only 1% Al present are very efficient for increasing the corrosion resistance (R_p), and the best R_p value was obtained after being immersed in the chloride solutions (3.5% NaCl) for 21 d. These fabricated coatings still show excellent corrosion resistance after prolonging the exposure period of time to 30 d in the test solution, but to a lower extent if compared to 21 d of their immersion.

4. Conclusions

In this study, three different coating formulations containing 1%, 2% and 3% Al particles were fabricated and characterized using different techniques: namely, SEM, TGA, pendulum hardness, scratch test and nano-indentation. The corrosion behaviour and the effect of adding the different Al percentages of the different manufactured coatings was reported after being immersed for 1 h, 7 d, 14 d, 21 d and 30 d in 3.5% NaCl solutions using the EIS measurements. It was found that the presence of 1% Al provides the best performance regarding the highest corrosion resistance after the various periods of exposure in the 3.5% NaCl solution. It was also found that prolonging the immersion time decreases the corrosion resistance after 7 d, but increasing the time of immersion to longer periods

of 14 d, 21 d and 30 d enhances the resistance to corrosion and reduces the degradation of the coated steel as a result of the formation of a surface layer corrosion product on the coatings. The obtained thermal and mechanical properties showed that the sample with the addition of 2% Al has the optimal conditions. On the other hand, the electrochemical results confirmed that the presence of 1% Al within the fabricated coating exhibits a higher corrosion resistance as compared to the coatings that have only 2% Al, while the addition of 3% Al provides the lowest corrosion resistance.

Author Contributions: Conceptualization, M.A.A., S.M.A.-Z. and E.-S.M.S.; Data curation, U.A.S.; Formal analysis, U.A.S. and J.A.M.; Investigation, M.A.A., J.A.M., S.M.A.-Z. and E.-S.M.S.; Methodology, M.A.A., U.A.S., A.H.S. and J.A.M.; Project administration, A.H.S.; Resources, A.H.S. and E.-S.M.S.; Software, U.A.S., J.A.M. and E.-S.M.S.; Supervision, A.H.S., S.M.A.-Z. and E.-S.M.S.; Visualization, M.A.A., S.M.A.-Z. and E.-S.M.S.; Writing—original draft, U.A.S. and E.-S.M.S.; Writing—review and editing, M.A.A., U.A.S., A.H.S., J.A.M., S.M.A.-Z. and E.-S.M.S. All authors have read and agreed to the published version of the manuscript.

Funding: This work was funded by the National Plan for Science, Technology and Innovation (MAARIFAH), King Abdul-Aziz City for Science and Technology, Kingdom of Saudi Arabia, grant number (2-17-02-001-0023).

Institutional Review Board Statement: Not applicable.

Informed Consent Statement: Not applicable.

Data Availability Statement: All the data are available within the manuscript.

Acknowledgments: This work was funded by the National Plan for Science, Technology and Innovation (MAARIFAH), King Abdul-Aziz City for Science and Technology, Kingdom of Saudi Arabia, grant number (2-17-02-001-0023).

Conflicts of Interest: The authors declare no conflict of interest.

References

1. Tjong, S.C.; Haydn, C. Nanocrystalline materials and coatings. *Mater. Sci. Eng. R Rep.* **2004**, *45*, 1–88. [\[CrossRef\]](#)
2. Andrievski, R.A. Films as Nanostructured Materials with Characteristic Mechanical Properties. *Mater. Trans.* **2001**, *42*, 1471. [\[CrossRef\]](#)
3. Galliano, F.; Landolt, D. Evaluation of corrosion protection properties of additives for waterborne epoxy coatings on steel. *Prog. Org. Coat.* **2002**, *44*, 217. [\[CrossRef\]](#)
4. Chopra, I.; Ola, S.K.; Priyanka; Dhayal, V.; Shekhawat, D.S. Recent advances in epoxy coatings for corrosion protection of steel: Experimental and modelling approach—A review. *Mater. Today Proc.* **2022**, *62*, 3. [\[CrossRef\]](#)
5. Rajgopalan, N.; Khanna, A.S. Effect of size and morphology on UV-blocking property of nanoZnO in epoxy coating. *Int. J. Sci. Res.* **2013**, *3*, 4.
6. Zhang, M.Q.; Rong, M.Z.; Yu, S.L.; Wetzel, B.; Friedrich, K. Improvement of tribological performance of epoxy by the addition of irradiation grafted nano-inorganic particles. *Macromol. Mater. Eng.* **2002**, *287*, 111. [\[CrossRef\]](#)
7. Shi, X.; Nguyen, T.A.; Suo, Z.; Liu, Y.; Avci, R. Effect of nanoparticles on the anticorrosion and mechanical properties of epoxy coating. *Surf. Coat. Technol.* **2009**, *204*, 237. [\[CrossRef\]](#)
8. Chattopadhyay, D.K.; Raju, K.V.S.N. Structural engineering of polyurethane coatings for high performance applications. *Prog. Polym. Sci.* **2007**, *32*, 352–418. [\[CrossRef\]](#)
9. Hare, C.H. Corrosion Control of Steel by Organic Coatings. In *Uhlig's Corrosion Handbook*; Revie, R.W., Ed.; John Wiley and Sons: Hoboken, NJ, USA, 2011; pp. 971–983.
10. Compère, C.; Fréchette, E.; Ghali, E. The corrosion evaluation of painted and artificially damaged painted steel panels by AC impedance measurements. *Corros. Sci.* **1993**, *34*, 1259–1274. [\[CrossRef\]](#)
11. Fedullo, N.; Sorlier, E.; Sclavons, M.; Bailly, C.; Lefebvre, J.-M.; Devaus, J. Polymer-based nanocomposites: Overview, applications and perspectives. *Prog. Org. Coat.* **2007**, *58*, 87–95. [\[CrossRef\]](#)
12. Yang, L.H.; Liu, F.C.; Han, E.H. Effects of P/B on the properties of anticorrosive coatings with different particle size. *Prog. Org. Coat.* **2005**, *53*, 91–98. [\[CrossRef\]](#)
13. Gonzáles, S.; Cáceres, F.; Fox, V.; Souto, R.M. Resistance of metallic substrates protected by an organic coating containing aluminum powder. *Prog. Org. Coat.* **2003**, *46*, 317–323. [\[CrossRef\]](#)
14. Tseluikin, V.N.; Koreshkova, A.A. Pulsed Electrodeposition of Composite Coatings Based on Zinc–Nickel Alloy. *Prot. Met. Phys. Chem. Surf.* **2018**, *54*, 453–456. [\[CrossRef\]](#)

15. Shourgeshty, M.; Aliofkhazraei, M.; Karimzadeh, A. Study on functionally graded Zn–Ni–Al₂O₃ coatings fabricated by pulse electrodeposition. *Surf. Eng.* **2019**, *35*, 167–176. [\[CrossRef\]](#)
16. Becker, O.; Varley, R.; Simon, G. Morphology, thermal relaxations and mechanical properties of layered silicate nanocomposites based upon high-functionality epoxy resins. *Polymer* **2002**, *43*, 4365. [\[CrossRef\]](#)
17. Gonzalez, S.; Rosca, I.C.M.; Souto, R.M. Investigation of the Corrosion Resistance Characteristics of Pigments in Alkyd Coatings on Steel. *Prog. Org. Coat.* **2001**, *43*, 282. [\[CrossRef\]](#)
18. Supplit, R.; Schubert, U.S. Corrosion Protection of Aluminum Pigments by Sol–Gel Coatings. *Corros. Sci.* **2007**, *49*, 3325–3332. [\[CrossRef\]](#)
19. Zhang, Y.; Ye, H.; Liu, H.; Han, K. Preparation and characterisation of aluminium pigments coated with silica for corrosion protection. *Corros. Sci.* **2011**, *53*, 1694–1699. [\[CrossRef\]](#)
20. Karbasi, A.; Moradian, S.; Tahmassebi, N.; Ghodsi, P. Achievement of optimal aluminum flake orientation by the use of special cubic experimental design. *Prog. Org. Coat.* **2006**, *57*, 175–182. [\[CrossRef\]](#)
21. Jalilia, M.; Rostamia, M.; Ramezanzadeh, B. An investigation of the electrochemical action of the epoxy zinc-rich coatings containing surface modified aluminum nanoparticle. *Appl. Surf. Sci.* **2015**, *328*, 95–108. [\[CrossRef\]](#)
22. Madhankumar, A.; Nagarajan, S.; Rajendran, N.; Nishimura, T. EIS evaluation of protective performance and surface characterization of epoxy coating with aluminum nanoparticles after wet and dry corrosion test. *J. Solid State Electrochem.* **2012**, *16*, 2085–2093.
23. Liang, Y.; Liu, F.-C.; Nie, M.; Zhao, S.; Lin, J.; Han, E.-H. Influence of Nano-Al Concentrates on the Corrosion Resistance of Epoxy Coatings. *J. Mater. Sci. Technol.* **2013**, *29*, 353–358. [\[CrossRef\]](#)
24. Alam, M.A.; Samad, U.A.; Seikh, A.; Mohammed, J.A.; Al-Zahrani, S.M.; Sherif, E.-S.M. Development and Characterization of PA 450 and PA 3282 Epoxy Coatings as Anti-Corrosion Materials for Offshore Applications. *Materials* **2022**, *15*, 2562. [\[CrossRef\]](#)
25. Samad, U.A.; Alam, M.A.; Chafidz, A.; Al-Zahrani, S.M.; Alharthi, N.H. Enhancing mechanical properties of epoxy/polyaniline coating with addition of ZnO nanoparticles: Nanoindentation characterization. *Prog. Org. Coat.* **2018**, *119*, 109–115. [\[CrossRef\]](#)
26. Samad, U.A.; Alam, M.A.; Sherif, E.S.M.; Alam, M.; Shaikh, H.; Alharthi, N.H.; Al-Zahrani, S.M. Synergistic effect of Ag and ZnO nanoparticles on polypyrrole-incorporated epoxy/2pack coatings and their corrosion performances in chloride solutions. *Coatings* **2019**, *9*, 287. [\[CrossRef\]](#)
27. Samad, U.A.; Alam, M.A.; Anis, A.; Abdo, H.S.; Shaikh, H.; Al-Zahrani, S.M. Nanomechanical and Electrochemical Properties of ZnO-Nanoparticle-Filled Epoxy Coatings. *Coatings* **2022**, *12*, 282. [\[CrossRef\]](#)
28. Azani, N.F.S.M.; Hussin, M.H. Comparison of cellulose nanocrystal (CNC) filler on chemical, mechanical, and corrosion properties of epoxy-Zn protective coatings for mild steel in 3.5% NaCl solution. *Cellulose* **2021**, *28*, 6523–6543. [\[CrossRef\]](#)
29. Kim, H.J.; Jung, D.H.; Jung, I.H.; Cifuentes, J.I.; Rhee, K.Y.; Hui, D. Enhancement of mechanical properties of aluminium/epoxy composites with silane functionalization of aluminium powder. *Compos. Part B Eng.* **2012**, *43*, 1743–1748. [\[CrossRef\]](#)
30. Oliver, W.C.; Pharr, G.M. An improved technique for determining hardness and elastic modulus using load and displacement sensing indentation experiments. *J. Mater. Res.* **1992**, *7*, 1564–1583. [\[CrossRef\]](#)
31. Vyazovkin, S. Modification of the integral isoconversional method to account for variation in the activation energy. *J. Comput. Chem.* **2001**, *22*, 178–183.
32. Nicodemo, L.; Nicolais, L. Mechanical properties of metal/polymer composites. *J. Mater. Sci. Lett.* **1983**, *2*, 201–203. [\[CrossRef\]](#)
33. Taşdemir, M.; Gülsoy, H.Ö. Mechanical Properties of Polymers Filled with Iron Powder. *Int. J. Polym. Mater.* **2008**, *57*, 258–265. [\[CrossRef\]](#)
34. Anis, A.; Elnou, A.Y.; Alam, M.A.; Al-Zahrani, S.M.; AlFayez, F.; Bashir, Z. Aluminum-Filled Amorphous-PET, a Composite Showing Simultaneous Increase in Modulus and Impact Resistance. *Polymers* **2020**, *12*, 2038. [\[CrossRef\]](#)
35. Feliu, S., Jr. Electrochemical impedance spectroscopy for the measurement of the corrosion rate of magnesium alloys: Brief review and challenges. *Metals* **2020**, *10*, 775. [\[CrossRef\]](#)
36. Uwaya, G.E.; Fayemi, O.E.; Sherif, E.M.; Junaedi, H.; Ebenso, E.E. Synthesis, electrochemical studies, and antimicrobial properties of Fe₃O₄ nanoparticles from callistemon viminalis plant extracts. *Materials* **2020**, *13*, 4894. [\[CrossRef\]](#) [\[PubMed\]](#)
37. AlOtaibi, A.A.; Sherif, E.-S.M.; Zinelis, S.; Al Jabbari, Y.S. Corrosion behavior of two cp titanium dental implants connected by cobalt chromium metal superstructure in artificial saliva and the influence of immersion time. *Int. J. Electrochem. Sci.* **2016**, *11*, 5877–5890. [\[CrossRef\]](#)
38. Sherif, E.M.; Park, S.-M. Effects of 1,5-Naphthalenediol on Aluminum Corrosion as a Corrosion Inhibitor in 0.50 M NaCl. *J. Electrochem. Soc.* **2005**, *152*, B205. [\[CrossRef\]](#)
39. Alam, M.A.; Sherif, E.-S.M.; Al-Zahrani, S.M. Mechanical Properties and Corrosion Behavior of Different Coatings Fabricated by Diglycidyl Ether of Bisphenol-A Epoxy Resin and Aradur®-3282 Curing Agent. *Int. J. Electrochem. Sci.* **2013**, *8*, 8388–8400.
40. Alam, M.A.; Samad, U.A.; Sherif, E.-S.M.; Seikh, A.; Al-Zahrani, S.M.; Alharthi, N.H.; Alam, M. Synergistic effect of Ag and ZnO nanoparticles on polyaniline incorporated epoxy/2pack coatings for splash zone applications. *J. Coat. Technol. Res.* **2019**, *16*, 835–845. [\[CrossRef\]](#)
41. Gopi, D.; Sherif, E.S.M.; Surendiran, M.; Sakila, D.A.; Kavitha, L. Corrosion inhibition by benzotriazole derivatives and sodium dodecyl sulphate as corrosion inhibitors for copper in ground water at different temperatures. *Surf. Interface Anal.* **2015**, *47*, 618–625. [\[CrossRef\]](#)

42. Fan, L.; Tang, F.; Reis, S.T.; Chen, G.; Koenigstein, M.L. Corrosion Resistances of Steel Pipes Internally Coated with Enamel. *Corrosion* **2017**, *73*, 1335–1345. [[CrossRef](#)] [[PubMed](#)]
43. Fan, L.; Reis, S.T.; Chen, G.; Koenigstein, M.L. Corrosion Resistance of Pipeline Steel with Damaged Enamel Coating and Cathodic Protection. *Coatings* **2018**, *8*, 185.
44. Mayne, J.E.O. The mechanism of the inhibition of the corrosion of iron and steel by means of paint. *Off. Dig.* **1952**, *24*, 127.
45. Samad, U.A.; Alam, M.A.; Anis, A.; Sherif, E.S.M.; Al-Mayman, S.I.; Al-Zahrani, S.M. Effect of Incorporated ZnO Nanoparticles on the Corrosion Performance of SiO₂ Nanoparticle-Based Mechanically Robust Epoxy Coatings. *Materials* **2020**, *13*, 3767. [[CrossRef](#)]
46. Davis, G.; Krebs, L.; Dacres, C. Coating evaluation and validation of accelerated test conditions using an in-situ corrosion sensor. *J. Coat. Technol.* **2002**, *74*, 69–74. [[CrossRef](#)]
47. Bacon, R.C.; Smith, J.J.; Rugg, F.M. Electrolytic resistance in evaluating protective merit of coatings on metals. *Ind. Eng. Chem.* **1948**, *40*, 161–167. [[CrossRef](#)]
48. Tsai, P.-Y.; Chen, T.-E.; Lee, Y.-L. Development and characterization of anticorrosion and antifriction properties for high performance polyurethane/graphene composite coatings. *Coatings* **2018**, *8*, 250. [[CrossRef](#)]
49. Kilpeläinen, V.; Gutierrez, A.; van Loon, S. Anticorrosive pigments—Properties of different talcs compared in corrosion testing. *Eur. Coat. J.* **2012**, *4*, 26.

Disclaimer/Publisher’s Note: The statements, opinions and data contained in all publications are solely those of the individual author(s) and contributor(s) and not of MDPI and/or the editor(s). MDPI and/or the editor(s) disclaim responsibility for any injury to people or property resulting from any ideas, methods, instructions or products referred to in the content.